

"© 2016 IEEE. Personal use of this material is permitted. Permission from IEEE must be obtained for all other uses, in any current or future media, including reprinting/republishing this material for advertising or promotional purposes, creating new collective works, for resale or redistribution to servers or lists, or reuse of any copyrighted component of this work in other works."

Inductive Charging Coupler with Assistive Coils

Shuo Wang¹, *Student Member*, David G. Dorrell¹, Youguang Guo¹ and Min-Fu Hsieh², *Senior Member, IEEE*

¹University of Technology Sydney, Broadway, NSW 2007, Australia

²National Cheng Kung University, Tainan 701, Taiwan

Wireless charging technology has been employed for many applications including high power applications, such as electric vehicle recharging, and low power applications such as biomedical device recharging or portal electronic devices. A wireless charging system contains a high frequency power source, a wireless transformer/coupler, a rectifier and the load. The wireless transformer/coupler is the key element of the wireless charging system. The performance and the power source and rectifier design are all dependent on the design of the wireless coupler. For a two coil type wireless transformer, the maximum efficiency is limited by the coupling coefficient which rapidly decreases with increasing distance between the primary and secondary coils. The four coil system is widely used in low power applications, where the maximum power transfer operating point is away from the maximum efficiency point. This paper proposes an inductive charging coupler with small assistive coils, where the high power and maximum efficiency regions overlap.

Index Terms— Inductive charging, eddy currents, medium frequency transformer, ac resistance, copper loss

I. INTRODUCTION

Wireless charging on an electric vehicle (EV) offers consumers another recharging option other than plug-in recharging. Since a manual connection between the grid and EV is not required by the wireless charger, it could be fully automatic. The conduction wire is replaced by a magnetic field between the EV and grid. This avoids the possibility of contact with any exposed charger components. Another advantage of wireless power transfer (WPT) is that it offers a greater recharging window. For stationary recharging, a recharging connection can be established in a few seconds, therefore it is possible to recharge the EV when waiting at traffic lights or travelling at a low speed in urban traffic. Dynamic WPT which supplies power when travelling at speed, is a long term goal for commercial EV.

The general structure of a wireless charging system is shown in Fig. 1. It has a high frequency (HF) power source, a wireless transformer, and a rectifier. Wireless recharging technology has three key areas: 1) wireless transformer design; 2) circuit configuration and power electronics design; and 3) system control.

The output frequency of the high frequency inverter ranges from 10 kHz to several tens of MHz. For many high power applications, such as EV wireless charging, the maximum efficiency is sought in order to reduce the recharging cost. A power source with a small impedance is preferred so that most of power can be transferred to the load. With the development of SiC and GaN devices, > 100 kHz inverters, which have low losses, are available for wireless charging applications. For low power applications, the impedance matching method is adopted to obtain the maximum power transfer [1].

For the wireless transformer design, the most common structures have two coils or four coils. In [2]-[7], two coil circular pads, I pads, DD pads, and DDQ pads, were employed. Circular pads have the same misalignment tolerance in all directions, while the DD and I pads have more misalignment tolerance in the forward and reverse directions.

Power transfer linkage is established by the WPT coupler, which is loosely coupled transformer. The coupling between the primary and secondary is low due to a large airgap.

In [8]-[12], four coil systems are used in low power devices. Impedance matching is used to acquire high power output. The transfer efficiency of the four coils system is high. However, many four coils system operate in MHz frequency range, in which the high efficiency low impedance power source currently is not available, causing a low total system efficiency. In [12], a four coil system for EV WPT with high total efficiency in 100 kHz was presented. The coaxial windings are used for both sides, but the high efficiency working point is away from the high power point. This means that extra redundancy is required for system design to transfer enough power around high efficiency point. And extra redundancy adds cost to both power electronics and transformer for using higher power rating devices and thicker wires. In this paper, an inductive charging coupler with separated small assistive coils is proposed. The frequency is 20 kHz to reduce the loss in power electronics as well as the eddy current in transformer. The proposed structure merges the high efficiency and high power output points. The coupling coefficient was analyzed using finite element analysis (FEA) and the power ratio was studied at circuit level. The simulation result is shown and compared with the same size two coil system.

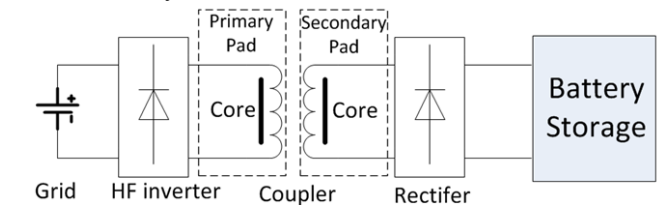


Fig. 1. Wireless charging circuit.

II. WIRELESS CHARGING SYSTEMS

A wireless transformer has a grid or power source primary coupler and secondary coupler which is connected to the vehicle battery charger. Generally, the primary coupler is isolated from secondary coupler. The electrical power will be transferred from the primary coupler to secondary coupler

across the airgap via a magnetic link. Many wireless transformer geometries have been proposed. The two coil structure has one winding on the primary side and one winding on the secondary side. Each winding can be formed by one or more coils connected in a series or parallel combination. For the four winding structure, there is an extra resonant coil or compensation coil in both the primary and secondary sides. The extra coils are short circuit or connected to a capacitor. Both the two winding and four winding structures are single phase applications. For single phase application, there can be multiple winding structures, but they can be treated as a combination of two or four winding systems. There is limited research on multi-phase structures. This is probably due to the complexities of a wireless transformer design and the control of the wireless charging system.

A. Two winding structure

The two coil system is widely used in inductive charging applications. The general structure is shown as in Fig. 1. Fig. 2 shows the equivalent circuit, where L_1 and L_2 are the inductances of the primary and secondary windings; C_1 and C_2 are the compensation capacitors and series-series (SS) capacitor compensation is used here; R_1 and R_2 are the total parasitic resistances of the windings and capacitors, and R_{load} is the load for the wireless charging system, respectively.

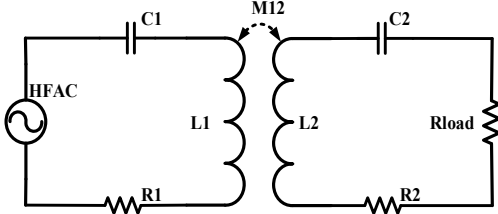


Fig. 2. General structure for series-series compensation.

The voltage equations can be written as

$$U = I_1 Z_1 + I_2 M \quad (1)$$

$$0 = I_1 M + I_2 Z_2 \quad (2)$$

where $Z_1 = R_1 + j\omega L_1 + \frac{1}{j\omega C_1}$

and $Z_2 = R_2 + R_L + j\omega L_2 - \frac{1}{j\omega C_1}$

Assuming that the inductance is fully compensated by the capacitor at the HFAC frequency $\omega L_1 = 1/\omega C_1$ then

$$U = \left[R_1 + \frac{(\omega M)^2}{R_2 + R_L} \right] I_1 \quad (3)$$

$$j\omega M_{12} Y_{11} U_1 = (R_{eq} + R_2 + R_L) I_2 \quad (4)$$

$$R_{eq} = R_1 + \frac{(\omega M)^2}{R_2 + R_L} \quad (5)$$

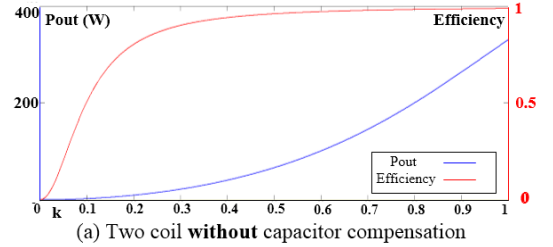
Therefore, the ratio between I_1 and I_2 is

$$\frac{|I_1|}{|I_2|} = \frac{(R_{eq} + R_2 + R_L)}{\omega M_{12} R_1 R_{eq}} = \frac{(R_{eq} + R_2 + R_L)}{k Q R_1 R_{eq}} \quad (6)$$

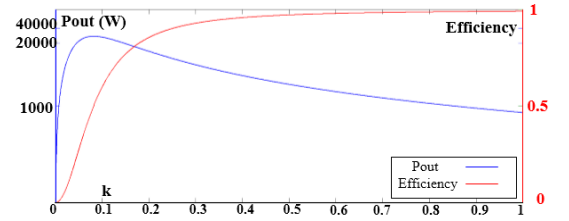
The efficiency of the two coils system is

$$\eta = \frac{I_2^2 R_L}{(I_2^2 (R_L + R_2) + I_1^2 R_1)} \quad (7)$$

Fig. 3 shows the simulation results (from a model developed in Ansys Maxwell 2D) for the efficiency and power output for variation of the coupling coefficient k . The system frequency is 20 kHz and the inductance is fully compensated with the capacitors. Both efficiency and power output, without the SS capacitors, decrease with decreasing coupling coefficient. The efficiency curve with SS compensation shows a similar trend but the output power is much higher than that without the SS capacitors when k is small. Since efficiency increases with the increasing k , the coupling coefficient is an important design parameter. For private-use EV wireless charging applications, the goal is to reach Level 1 or Level 2 charging, which is 1 to 6.6 kW, with the highest efficiency possible. Due to practical considerations, such as the limitation of the coupler size and essential gap between ground and vehicle, the coupling coefficient is between 0.1 to 0.3 from most published studies.



(a) Two coil **without** capacitor compensation



(b) Two coil circuit **with** SS capacitor compensation

Fig. 3. Simulation results

B. Four winding structure

The four coil system was reported in [11]. Impedance matching between the input and output is applied to acquire the maximum power output in low power applications, which often have a system efficiency lower than 50%. In [12], a four coil system is used for EV wireless charging, in which the maximum efficiency principle is used. There is still a power-efficiency split in the coaxial coil coupler where the maximum power and efficiency cannot be reached at the same time. The general structure of four winding system is shown in Fig. 4.

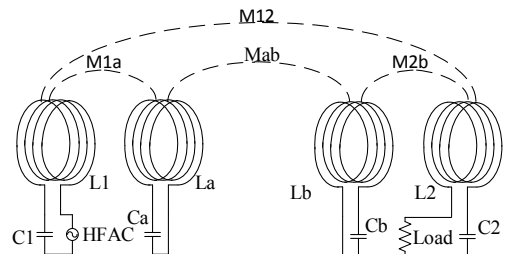


Fig. 4. General structure for four coil system.

The system is driven by a high frequency power source. The circuit equation matrix for a four coil system is

$$\begin{bmatrix} U_0 \\ 0 \\ 0 \\ 0 \end{bmatrix} = \begin{bmatrix} Z_1 & M_{12} & M_{13} & M_{14} \\ M_{21} & Z_2 & M_{23} & M_{24} \\ M_{31} & M_{32} & Z_3 & M_{34} \\ M_{41} & M_{42} & M_{43} & Z_4 \end{bmatrix} \begin{bmatrix} I_1 \\ I_2 \\ I_3 \\ I_4 \end{bmatrix} \quad (8)$$

where

$$Z_{1,2,3} = r_{w1,w2,w3} + j\omega L_{1,2,3} - 1/j\omega C_{1,2,3} \quad (9)$$

$$Z_4 = r_{w4} + j\omega L_4 - 1/j\omega C_4 + R_{load}$$

and M is the mutual inductance between two coils. The power output to the load is

$$P_{out} = |I_4|^2 R_{load} \quad (10)$$

The efficiency of the four coil system is

$$\eta = \frac{P_{out}}{P_{out} + P_{loss}} = \frac{|I_4|^2 R_{load}}{|I_4|^2 R_{load} + \sum_{i=1}^4 |I_i|^2 R_{wi}} \quad (11)$$

III. PROPOSED COUPLER WITH ASSISTIVE COILS

Since the wireless transformer is a loosely coupled transformer, the leakage flux is high. In order to reduce this, the magnetic field needs to be modified so that the flux linkage between two sides is increased and the leakage is reduced. To do this, a coupler with assistive coils is proposed, and this is shown in Fig. 5. Fig. 5(a) shows a 3D view, while Fig. 4(b) shows the top view of the primary coupler and 4(c) shows a side view. Each side of the coupler has the major coil, four small assistive coils, and ferrite, which is used to help the flux linkage. The four assistive coils are connected in series or parallel, forming an assistive winding, which makes it a four coil system. In this paper, the SS connected compensation is analyzed.

This transformer is simulated in the ANSYS Maxwell 3D. The parameters for the transformer are shown in Table I. The frequency of the system is set to 20 kHz, therefore, the ferrite and Litz-Wire are used to reduce the transformer eddy current loss.

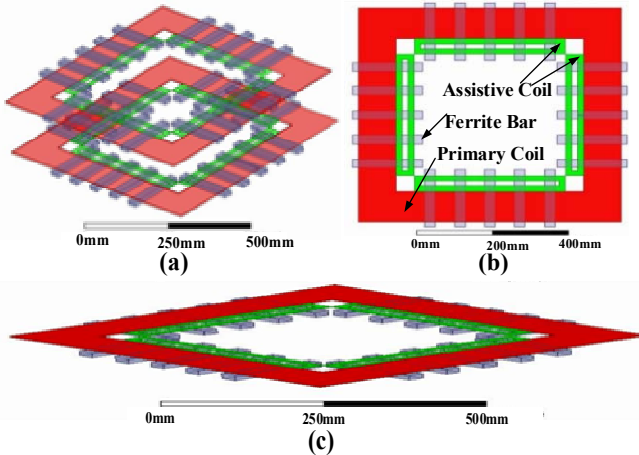


Fig. 5. General structure for four coil system: a) 3D view of transformer; b) top view of primary coupler; c) side view of primary coupler.

TABLE I. PARAMETERS OF SIMULATED COUPLER

Coil/Ferrite	Length [mm]	Turns
Coil 1-2	700×700	10
Coil a-b	400×48	10
Ferrite bar	186×28×16	n/a

IV. CIRCUIT MODEL FOR PROPOSED COUPLER

Fig. 6 shows the circuit model for the coupler with the assistive coils. Four small coils on the primary side are series connected and form the assistive coil La. The secondary side has the assistive coil Lb. La and Lb are connected to capacitors Ca and Cb, respectively. The high frequency power is connected to the primary coil L1 and compensation capacitor C1. The load is series connected to the secondary coil L2 via capacitor C2. The mutual inductances between coils are shown as M1a, M12, M1b, M2a, M2b, Mab. Mab is the mutual inductance between coils a and b.

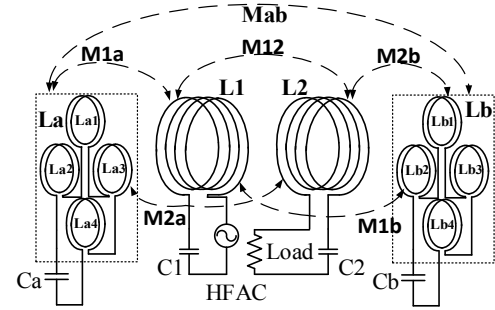


Fig. 6. Circuit model for proposed coupler with assistive coil system.

V. SIMULATION RESULTS

A. FEA simulation result

The inductance matrix of the proposed system was simulated. The airgap distance between the primary and secondary coils is set to 200 mm in the FEA simulation, which is almost 1/3 of the transformer length. The inductance matrix from the FEA simulation is shown in Table II, and the coupling coefficient matrix is shown in Table III.

TABLE II. INDUCTANCE MATRIX OF FOUR COILS

Inductances [μ H]	Coil 1	Coil 2	Coil 3	Coil 4
Coil 1	160	39.012	6.835	36.975
Coil 2	39.012	198.42	1.555	6.832
Coil 3	6.8352	1.555	198.42	38.993
Coil 4	36.975	6.832	38.993	160

TABLE III. COUPLING COEFFICIENT MATRIX

k	Coil 1	Coil 2	Coil 3	Coil 4
Coil 1	1	0.218	0.0383	0.230
Coil 2	0.218	1	0.00784	0.0382
Coil 3	0.038	0.00784	1	0.219
Coil 4	0.230	0.0383	0.21851	1

For different working conditions, the airgap length varies. The coupling coefficient k for varying airgap length is shown in Fig. 7. The coupling between the primary and secondary windings decreases with increasing airgap. The k_{1a} between windings 1 and a is almost constant when the airgap is large. k_{1a} is high when the airgap is relatively small, which may be

affected by the secondary side winding and ferrite. k_{2a} decreases with the separation and its values are small beyond 150 mm which means the coupling between the major coil and the assistive windings is weak.

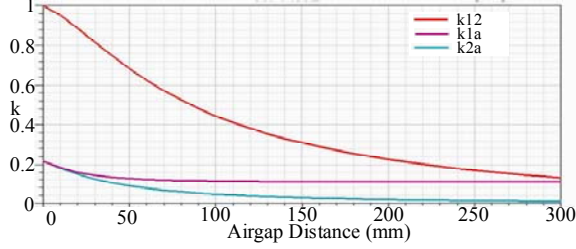


Fig. 7. Coupling coefficient via airgap length.

B. Circuit Analysis

With an ideal high frequency power source, the compensation capacitor affects the system characteristic. To estimate the output power and efficiency, it is important to simulate the compensation characteristic of the two coil system and proposed system. The circuit model in Section II.a is simulated for the two coil system and the circuit model in Section II.b is simulated for the proposed system. Both 700mm square pads are used for two coil and proposed pad. The resonant capacitances for each winding at 20 kHz are normalized as C_{1r} , C_{2r} , C_{3r} , and C_{4r} .

1) Two coil system with SS compensation

The performance of the two coil system is different with different capacitor compensation connection. The series-series compensation is employed in both two coil and proposed system for comparison.

The output frequency of the power source is set to 20 kHz. The inductance matrix in Table II for a 700 mm square pad with 150 mm airgap is used for the simulations. In the two coil system, there are only primary coil and secondary coil capacitors, which are C_1 and C_4 for the convenience of comparison to the proposed four coil system. The winding resistance is set to 0.09Ω for all the windings.

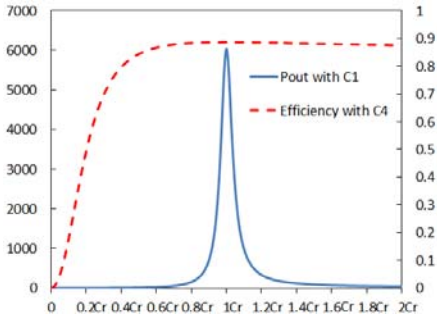


Fig. 8. Two coil system Characteristic with C_1 and C_4 .

The dash line in Fig. 8 shows the two coil system efficiency with the change of C_4 when primary side is well compensated and the solid line shows the power output with the change of C_1 when secondary side is well compensated. Both maximum power and efficiency are reached around the L_1/C_1 and L_4/C_4 resonance point in simulated system. However, the maximum overall system efficiency is lower than 0.9 in the two coil

system.

2) Four coil system with SS compensation

The capacitor for the primary coil is C_1 , and the primary assistive coil is C_2 . The secondary assistive coil is C_3 and secondary coil is C_4 .

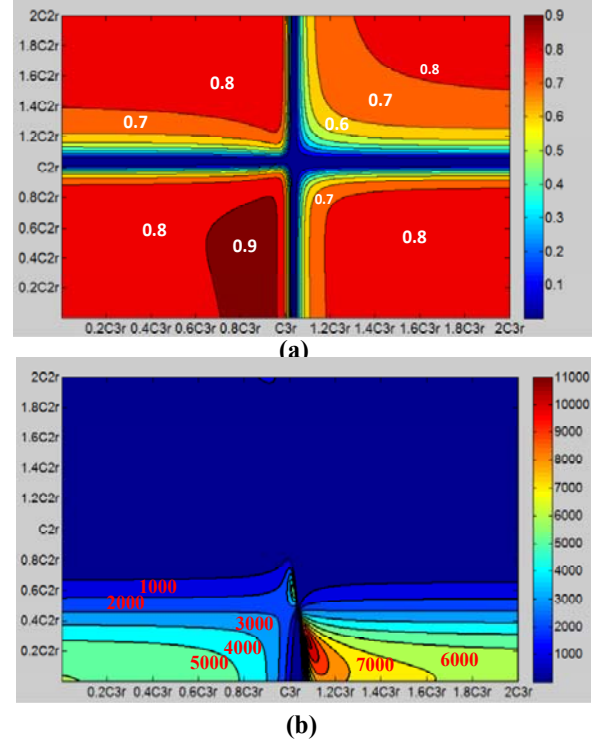


Fig. 9. Proposed coupler optimization.

In the proposed system, the maximum overall efficiency is over 0.94, as illustrated in Fig. 9. When the assistive coils are well tuned at resonance at source frequency, higher power would be transferred to the assistive coil comparing to the load side. And the power would be consumed by the parasitic resistance which causes cross-shaped low efficiency region in Fig. 9a).

The highest efficiency region is on the left bottom close to C_{3r} . The highest power transfer region, which reaches 11 kW, is on the right bottom close to C_{3r} . The highest efficiency region can transfer 1 to 5 kW, which is sufficient for a level 1 or 2 EV charger. The primary compensation capacitor has a high impact on power transferred to the secondary side because only part of the flux generated by the primary coil is captured by the secondary coil. Therefore the power map is not symmetrical.

The maximum power-maximum efficiency regions are still away from each other, but in the maximum efficiency region, the transferred power is between $1/3^{\text{rd}}$ and $1/2^{\text{nd}}$ of the maximum transferred power. The two regions are closer compared to the coaxial four coil system.

VI. CONCLUSIONS

In order to transfer power to an EV with high efficiency, the wireless transformer needs to be designed correctly. The circuit model for two coil and four coil systems are shown. A coupler with assistive coils is proposed. The simulation results

show that the efficiency of the proposed system is higher than the simulated two coil system. The proposed system is capable of transferring 1 to 5 kW power with over 90% efficiency. The future work is to develop an analytical model for the coupler, which would give a detailed explanation and understanding for the proposed IPT pad.

REFERENCES

- [1] S. Y. R. Hui, W. X. Zhong, C. K. Lee, "A critical review of recent progress in mid-range wireless power transfer," *IEEE Trans. on Power Electron.*, 2013, DOI: 10.1109/TPEL.2013.2249670.
- [2] W. Chwei-Sen, O. H. Stielau, and G. A. Covic, "Design considerations for a contactless electric vehicle battery charger," *IEEE Trans. on Industrial Electronics*, vol. 52, pp. 1308-1314, 2005.
- [3] M. Budhia, J. T. Boys, G. A. Covic, and H. Chang-Yu, "Development of a single-sided flux magnetic coupler for electric vehicle IPT charging systems," *IEEE Trans. on Ind. Electr.*, vol. 60, pp. 318-328, 2013.
- [4] S. Wang and D. G. Dorrell, "Loss analysis of circular wireless EV charging coupler," *IEEE Trans. on Magn.*, vol. 50, no. 11, Article#: 8402104, 2014.
- [5] S. Wang and D. G. Dorrell, "Review of wireless charging coupler for electric vehicles," *IEEE IECON Conference*, Vienna, Nov 2013.
- [6] F. Musavi, M. Edington, and W. Eberle, "Wireless power transfer: A survey of EV battery charging technologies," *IEEE ECCE*, 2012, pp. 1804-1810.
- [7] G. A. Covic, L. G. Kissin, D. Kacprzak, N. Clausen, and H. Hao, "A bipolar primary pad topology for EV stationary charging and highway power by inductive coupling," *IEEE ECCE*, Sep. 2011, pp. 1832-1838.
- [8] Y. H. Kim, S. Y. Kang, S. Cheon, M. L. Lee, J. M. Lee, and T. Zyung, "Optimization of wireless power transmission through resonant coupling," *SPEEDAM*, 2010, pp. 1069-1073.
- [9] S. Cheon, Y. H. Kim, S. Y. Kang, M. L. Lee, J. M. Lee, and T. Zyung, "Circuit-model-based analysis of a wireless energy-transfer system via coupled magnetic resonances," *IEEE Trans. Ind. Electron.*, vol. 58, no. 7, pp. 2906-2914, Jul. 2011.
- [10] P. Si, A. P. Hu, J. W. Hsu, M. Chiang, Y. Wang, S. Malpas, and D. Budgett, "Wireless power supply for implantable biomedical device based on primary input voltage regulation," *2nd IEEE Conf. Ind. Electron. Appl.*, May 2007, pp. 235-239.
- [11] A. Kurs, A. Karalis, R. Moffatt, J. D. Joannopoulos, P. Fisher, and M. Soljacic, "Wireless power transfer via strongly coupled magnetic resonances," *Science*, vol. 317, no. 5834, pp. 83-86, Jul. 2007.
- [12] Q. Zhu, L. Wang, and C. Liao, "Compensate capacitor optimization for kilowatt-level magnetically resonant wireless charging system," *IEEE Trans. Ind. Electron.*, vol. 61, no. 12, pp. 6758-6768, Dec. 2014.
- [13] S. Wang and D. G. Dorrell, "Copper Loss Analysis of EV Charging Coupler," *IEEE Trans. on Magn.*, vol. 51, no. 11, pp. 1-4, Nov. 2015.